From the Archives of the AFIP

This article meets the criteria for 1.0 credit hour in category 1 of the AMA Physician's Recognition Award. To obtain credit, see the questionnaire on pp 1239-1246.

LEARNING OBJECTIVES

After reading this article and taking the test, the reader will:

- Be familiar with the spectrum of radiologic appearances of enchondroma and intramedullary chondrosarcoma involving the appendicular skeleton.
- Understand the pathologic basis of the radiologic findings of enchondroma and intramedullary chondrosarcoma affecting the appendicular skeleton.
- Be familiar with the radiologic manifestations that allow differentiation of the majority of enchondromas and intramedullary chondrosarcomas affecting the appendicular skeleton.

Enchondroma versus Chondrosarcoma in the Appendicular Skeleton: Differentiating Features[1]

Mark D. Murphey, MD • Donald J. Flemming, CDR, MC, USN • Steven R. Boyea, MAJ, MC, USA • John A. Bojescul, CPT, MC, USA • Donald E. Sweet, MD • H. Thomas Temple, MD[2]

Distinction of enchondroma versus intramedullary chondrosarcoma affecting the appendicular skeleton (proximal to the metacarpals and metatarsals) is a frequent diagnostic dilemma. The authors studied a large series of patients with these lesions (92 with enchondromas, 95 with chondrosarcomas) using statistical assessment of both clinical parameters and numerous radiologic manifestations on images from multiple modalities to identify differentiating features. Multiple clinical and imaging parameters demonstrated statistically significant differences between enchondroma and chondrosarcoma, particularly pain related to the lesion, deep endosteal scalloping (greater than two-thirds of cortical thickness), cortical destruction and soft-tissue mass (at computed tomography or magnetic resonance imaging), periosteal reaction (at radiography), and marked uptake of radionuclide (greater than the anterior iliac crest) at bone scintigraphy. All of these features strongly suggested the diagnosis of chondrosarcoma. These criteria allow distinction of appendicular enchondroma and chondrosarcoma in at least 90% of cases.

Index terms: Bone neoplasms, 41.3114, 41.3211, 45.3114, 45.3211 • Bone neoplasms, diagnosis • Enchondroma, 41.3114, 45.3114 • Sarcoma, 41.3211, 45.3211

RadioGraphics 1998; 18:1213-1237

[1]From the Departments of Radiologic Pathology (M.D.M.) and Orthopedic Pathology (D.E.S.), Armed Forces Institute of Pathology, Bldg 54, Rm M-121, 16th and Alaska Sts, NW, Washington DC 20306-6000; Departments of Radiology and Nuclear Medicine (M.D.M., D.J.F.) and Surgery (H.T.T.), Uniformed Services University of the Health Sciences, Bethesda, Md; Department of Radiology, University of Maryland School of Medicine, Baltimore (M.D.M.); Department of Radiology, National Naval Medical Center, Bethesda, Md (D.J.F.); and Department of Orthopedic Surgery, Walter Reed Medical Center, Washington DC (S.R.B., J.A.B., H.T.T.). Presented as a scientific paper at the 1996 RSNA scientific assembly. Received April 23, 1998; revision requested June 1 and received June 22; accepted June 23. **Address reprint requests to** M.D.M.

The opinions or assertions contained herein are the private views of the authors and are not to be construed as official nor as reflecting the views of the Departments of the Army, Navy, or Defense.

[2]Current address: Department of Orthopedic Surgery, University of Virginia School of Medicine, Charlottesville.

■ INTRODUCTION

Enchondroma and intramedullary chondrosarcoma (hence referred to as chondrosarcoma) are common chondroid musculoskeletal neoplasms representing 3%-17% and 8%-17% of primary bone tumors at biopsy series, respectively (1;2, pp 25-47, 71-109;3-5;6, pp 213-224, 267-304;7, pp 268-276, 343-366). Enchondromas are the result of the continued growth of residual benign cartilaginous rests that are displaced from the growth plate. They are particularly frequent, being recognized in 1.7% of femora at autopsy series (8,9). Distinction between these two lesions is important because of differences in patient management and outcome.

Enchondromas are most common in the hands or feet (phalanges, metacarpals, and metatarsals), and in these locations chondrosarcoma is exceedingly rare so that clinically these cartilage lesions do not present a diagnostic dilemma (3;6, pp 213-224;10, pp 3697-3711). Similarly, chondrosarcomas are common in the axial skeleton (spine and pelvis), typically with large associated soft-tissue masses, whereas enchondromas are very unusual in this location, again leading to obvious clinical differentiation (3;6, pp 213-224;10, pp 3746-3757). In fact, in our initial review of over 400 of these lesions, we found only one solitary enchondroma of the pelvis. However, differentiation of enchondroma from chondrosarcoma in the appendicular skeleton is often difficult clinically, radiologically, and pathologically (11-15).

The difficulty in distinguishing these lesions radiologically reflects the histologic heterogeneity of chondrosarcomas, which can display bland-appearing cartilage cells similar to those found in enchondroma in one area and foci of low- to intermediate-grade malignancy in other regions (16-20). Radiologic recognition of chondrosarcoma is vital in clinical management of patients, since it allows identification of those lesions which warrant biopsy and since it helps direct the surgeon to the most aggressive region and thereby avoid sampling error. Surgical management of these two lesions is also dramatically different, with intralesional curettage being used for symptomatic enchondroma versus wide resection for higher-grade chondrosarcoma. The latter lesion is associated with local recurrence and metastases with reduced life expectancy (16,17). Although radiography is often diagnostic in the assessment of many bone tumors, a limited number of previous investigations suggest that discrimination of benign from malignant cartilage lesions is more difficult (21-42). However, many of these studies have included only small numbers of patients and anatomic areas in which typically there is no clinical difficulty in distinguishing these lesions (hands, feet, and pelvis) and have not evaluated multiple imaging modalities with quantitative assessment of varying parameters (21-40). Radiologists, in our experience, are often asked by pathologists and referring clinicians to help in the differentiation between these lesions, and many standard bone neoplasm pathology texts suggest the use of imaging in this assessment but provide little guidance as to the important distinguishing features.

Our purpose in this study was to identify statistically significant differentiating clinical and imaging features of enchondroma and chondrosarcoma in a large population of pathologically proved lesions. The imaging features were based on evaluation of multiple radiologic studies including radiography, bone scintigraphy, computed tomography (CT), and magnetic resonance (MR) imaging. We limited our study to evaluation of enchondromas and chondrosarcomas of the appendicular skeleton excluding the phalanges, metacarpals, and metatarsals to assess more closely the typical clinical dilemma.

■ MATERIALS AND METHODS

This retrospective study was based on a review of the patient charts and imaging studies of all patients with a diagnosis of either enchondroma (n = 92) or chondrosarcoma (n = 95) of the appendicular skeleton, excluding phalanges, metacarpals, or metatarsals, from our institutions. All 187 cases were either pathologically proved (n = 172) or presumptively diagnosed as enchondroma (n = 15) based on follow-up assessment without clinical or radiologic change for at least 5 years. Only patients

with adequate documentation of clinical history, solitary intramedullary lesions (patients with Ollier or Maffucci syndromes were excluded), and at least two imaging studies (including radiography, bone scintigraphy, CT, or MR imaging) available for review were included.

Enchondromas were histologically defined as lesions with cellularity that exceeds resting articular cartilage, small nuclei, uniform nucleoli, and abundant cytoplasm. Mitotic activity was absent or very rare, although limited binucleate lacunae may be seen. Chondrosarcoma was divided histologically into three grades, and perhaps its most important distinction from enchondroma was the infiltration and entrapment of normal trabecular bone. Grade 1 chondrosarcoma had increased and focal atypical cellularity with occasional binucleate cells and focal trabecular entrapment. Grade 2 chondrosarcoma showed increased cellularity with diffuse cellular atypia, hyperchromatosis, and myxoid changes. Grade 3 chondrosarcomas were hypercellular with marked atypia but without cartilage lobules and demonstrated sheetlike growth coursing between residual trabecular bone.

Clinical assessment included patient age, sex, the presence or absence of symptoms including pain, and lesion location.

Radiologic studies were reviewed by two experienced musculoskeletal radiologists (M.D.M., D.J.F.) and one orthopedic oncologist (H.T.T.) without knowledge of the clinical history or final diagnosis (enchondroma vs chondrosarcoma) and included radiography (n = 187, 92 enchondromas and 95 chondrosarcomas), CT (n = 88, 39 enchondromas and 49 chondrosarcomas), MR imaging (n = 68, 35 enchondromas and 33 chondrosarcomas), and bone scintigraphy (n = 118, 67 enchondromas and 51 chondrosarcomas). Final evaluation was made by consensus among the three observers. Radiographs, CT scans, and MR images were evaluated for lesion size and location (central; eccentric; epiphysis, metaphysis, or diaphysis of lesion center), as well as the presence or absence of the following characteristics: endosteal scalloping, cortical remodeling (expansion of normal bone contour), cortical destruction, mineralized matrix, pathologic fracture, periosteal reaction, cortical thickening, and soft-tissue extension.

Endosteal scalloping was further classified by both extent and depth, with no scalloping present being grade 0. Extent of endosteal scalloping was graded as grade 1, involving less than one-third of the lesion extent; grade 2, affecting between one-third and two-thirds of lesion extent; and grade 3, involving greater than two-thirds of the lesion. Depth of endosteal scalloping was also graded and determined by the most prominent location (if any) and classified as grade 1, representing less than one-third of cortical thickness; grade 2, between one-third and two-thirds; grade 3, greater than two-thirds; and grade 4, cortical penetration (with or without associated soft-tissue mass).

Mineralized matrix was assessed on radiographs, CT scans, and MR images as present or absent, as subtle or obvious, and for its extent (grade 1, in less than one-third of the lesion length; grade 2, in more than one-third but less than two-thirds of the lesion; and grade 3, in greater than two-thirds of the lesion). On MR images obtained with all pulse sequences, mineralized matrix was considered to represent globular areas of low signal intensity. The intrinsic characteristics of mineralized matrix were further evaluated only on radiographs and CT scans as arcs and rings or flocculent in appearance.

In addition, CT scans were evaluated for the size of the soft-tissue component and the attenuation characteristics of the nonmineralized component (homogeneous; heterogeneous; lower than, similar to, or higher than that of muscle).

MR images were also evaluated for the presence of small high-signal-intensity foci with T1 weighting, lobulated lesion margin, and size of any soft-tissue component and its signal-intensity characteristics (homogeneous; heterogeneous; low, intermediate, or high signal intensity) with both T1 and T2 weighting. MR images obtained after intravenous administration of gadolinium-based contrast material (n = 30 enchondromas, n = 9 chondrosarcomas) were also assessed for the degree (mild, moderate, or marked) and predominant pattern (septal, peripheral, or diffuse) of enhancement.

Table 1
Demographics, Lesion Size, and Lesion Location in Patients with Enchondromas versus Those with Chondrosarcomas

Parameter	Enchondroma (n = 92)	Chondrosarcoma (n = 95)
Patient demographics		
Sex		
Male	36 (39)	52 (55)
Female	56 (61)	43 (45)
Age (y)*	8-76 (40)	9-86 (50)
Pain symptoms (%)	79	95
Lesion size (cm)*		
Radiography	2-16 (6.7)	1-28 (10.0)
CT	2-18 (5.0)	3-26 (8.0)
MR imaging	3-16 (5.0)	3-28 (8.0)
Skeletal distribution		
Femur	48 (52)	54 (57)
Humerus	26 (28)	20 (21)
Tibia	8 (9)	13 (14)
Fibula	6 (7)	3 (3)
Osseous location†		
Epiphysis	3 (3)	14 (16)
Metaphysis	34 (39)	44 (49)
Diaphysis	51 (58)	32 (36)

Note.—Numbers in parentheses are percentages except where otherwise indicated.
*Numbers in parentheses are mean values.
†Excludes lesions in flat bones.

Bone scintigrams were graded both for degree and extent of radionuclide uptake. The degree of radionuclide uptake (on whole-body image if possible) was compared with that in the anterior iliac crests. Radionuclide uptake in the lesion less than that of the anterior iliac crest was grade 1; similar to the anterior iliac crest, grade 2; and greater than the anterior iliac crest, grade 3. The extent of radionuclide uptake was compared with lesion length on radiographs as similar, larger, or smaller. The radionuclide activity was also assessed as homogeneous or heterogeneous. Finally, dynamic and blood pool images (when available) were assessed for the presence or absence of radionuclide uptake and its degree (mild, moderate, or marked).

The results for enchondromas and chondrosarcomas were compared by using the two-sample t test for continuous variables (ie, age and lesion size), Wilcoxon-Mann-Whitney rank sum test for graded variables, and Fisher exact test (two-tailed) for dichotomous data (43). Odds ratios from the univariate analyses were calculated, together with 95% confidence intervals. Data were analyzed by using SPSS 8.0 for Windows (SPSS, Chicago, Ill).

■ RESULTS

Patient demographics, pain symptoms, and the most frequent locations of enchondroma and chondrosarcoma are shown in Table 1. These lesions were statistically significantly different in terms of patient age (P = .007), sex (P = .04), and the presence of pain (P = .002). A mass was palpable in 28% of enchondromas and 82% of chondrosarcomas (P = .004). Additional clinical signs of weight loss, reduced joint motion, or symptom duration were not significantly different between the two lesions. The femur was the most commonly affected site for both lesions, although enchondromas more frequently occurred distally (36% of cases) and chondrosarcoma, proximally (34% of cases).

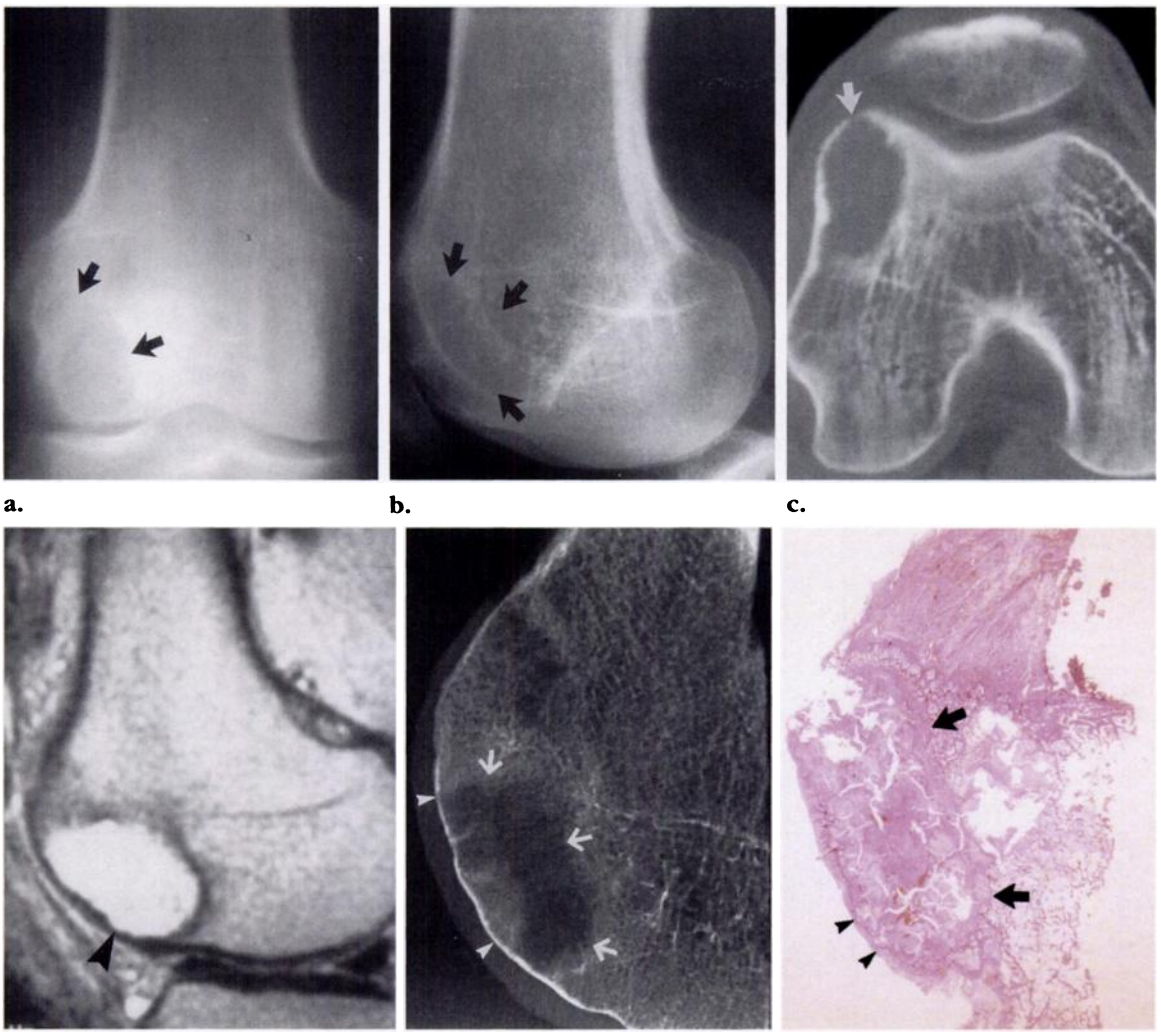

Figure 1. Chondrosarcoma of the distal femoral epiphysis in a 41-year-old man with knee pain. **(a, b)** Anteroposterior **(a)** and lateral **(b)** radiographs of the right knee show a lytic epiphyseal lesion (arrows) in the lateral femoral condyle that extends down to the joint surface. **(c)** Axial CT scan demonstrates the lesion, which is nonmineralized, but focal scalloping (arrow) of the anterior cortex, not appreciated on radiographs, is seen. Grading of scalloping is difficult because of normal thinning of the cortex in this region. **(d)** On a sagittal T2-weighted (repetition time msec/echo time msec = 2,000/80) MR image, the lesion is hyperintense, and focal endosteal scalloping (arrowhead) is appreciated. **(e, f)** Radiograph **(e)** and photograph **(f)** of sagittally sectioned whole mount specimen (hematoxylin-eosin stain) show the lesion (arrows) and focal endosteal scalloping (arrowheads).

There was no statistically significant difference between neoplasms in terms of specific lesion site. Lesions also varied in their longitudinal location in bone as shown in Table 1, with chondrosarcomas most frequently centered in the epiphysis ($P = .009$) (Fig 1) or metaphysis ($P = .236$), whereas enchondromas were more common in the diaphysis ($P = .003$). Lesion size was mildly greater on radiographs (Table 1) compared with their size on CT scans and MR images. The average size of enchondromas on CT and MR images was 5.0 cm (range, 2–18 cm) versus 8.0 cm (range, 3–28 cm) for chondrosarcomas ($P = .001$ at radiography, .04 at CT, and .008 at MR imaging).

Table 2
Depth of Endosteal Scalloping in Enchondromas and Chondrosarcomas as Depicted by Modality

Scalloping Depth*	Enchondroma	Chondrosarcoma
Radiography (n = 92, n = 95)†		
Grade 0	32 (35)	8 (8)
Grade 1	36 (39)	9 (9)
Grade 2	16 (17)	7 (7)
Grade 3	6 (7)	20 (21)
Grade 4	2 (2)	51 (54)
CT (n = 39, n = 49)†		
Grade 0	7 (18)	2 (4)
Grade 1	24 (62)	2 (4)
Grade 2	4 (10)	1 (2)
Grade 3	3 (8)	7 (14)
Grade 4	1 (3)	37 (76)
MR imaging (n = 35, n = 33)†		
Grade 0	16 (46)	3 (9)
Grade 1	14 (40)	1 (3)
Grade 2	3 (9)	1 (3)
Grade 3	1 (3)	4 (12)
Grade 4	1 (3)	24 (73)

Note.—Numbers in parentheses are percentages.
*Grade 0 = no scalloping, grade 1 = less than one-third of cortical thickness, grade 2 = one-third to two-thirds of cortical thickness, grade 3 = more than two-thirds of cortical thickness, grade 4 = cortical penetration.
†n = number of studies available for each lesion type (with number for enchondromas given first and chondrosarcoma, second). $P < .0005$.

Table 3
Extent of Endosteal Scalloping in Enchondromas and Chondrosarcomas as Depicted by Modality

Scalloping Extent*	Enchondroma	Chondrosarcoma
Radiography†		
Grade 1	25 (42)	14 (16)
Grade 2	16 (27)	11 (13)
Grade 3	19 (32)	62 (71)
CT†		
Grade 1	8 (25)	5 (11)
Grade 2	13 (41)	5 (11)
Grade 3	11 (34)	37 (79)
MR imaging†		
Grade 1	17 (89)	4 (13)
Grade 2	0 0)	6 (20)
Grade 3	2 (11)	20 (67)

Note.—Data are given only for those cases in which scalloping was present. Numbers in parentheses are percentages, which were calculated from total for each modality.
*Grade 1 = involving less than one-third of lesion extent, grade 2 = involving one-third to two-thirds of lesion extent, grade 3 = involving more than two-thirds of lesion extent.
†$P < .0005$.

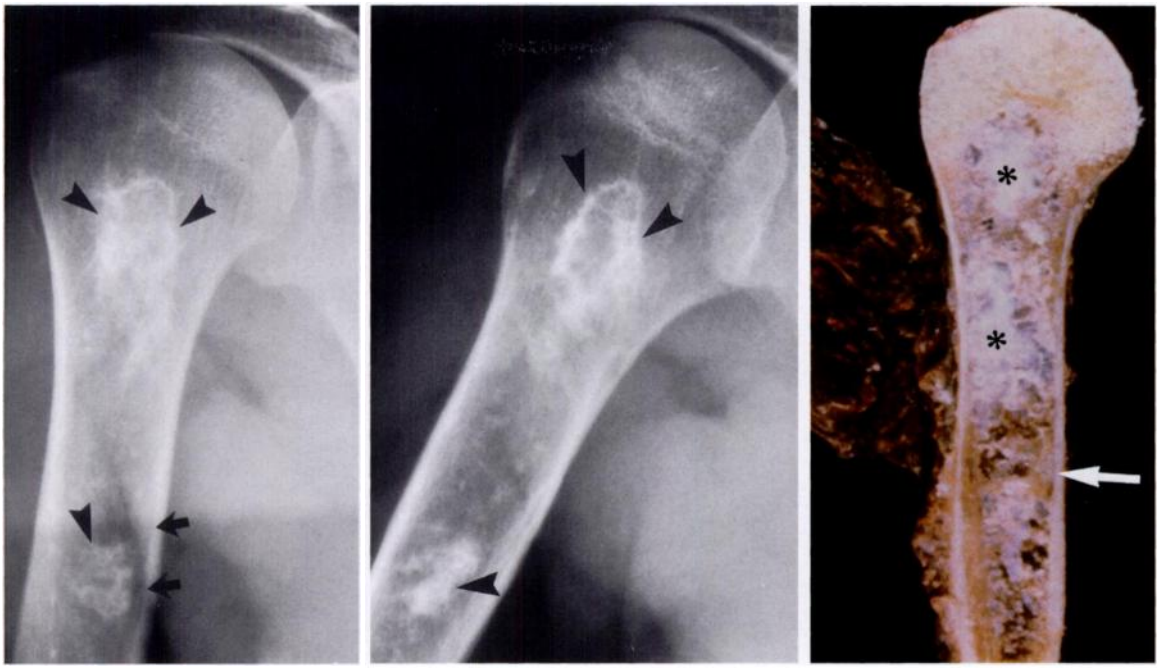

a. b. c.

Figure 2. Enchondroma of the humerus in a 53-year-old man with dull aching pain for 2 years. **(a, b)** Anteroposterior radiographs of the right shoulder in external **(a)** and internal **(b)** rotation show a lesion with arcs and rings pattern of mineralized chondroid matrix (arrowheads) involving the proximal humeral metadiaphysis. Endosteal scalloping (arrows in **a**) that is focal and shallow (less than one-third cortical thickness and along less than one-third lesion extent) is seen at the inferomedial aspect of the lesion. **(c)** Photograph of coronally sectioned gross specimen demonstrates a lobular growth pattern and white chondroid matrix (*). Focal shallow endosteal scalloping (arrow) correlates well with the imaging appearance.

Depth and extent of endosteal scalloping at radiography, CT, and MR imaging and associated *P* values are shown in Tables 2 and 3 (Figs 1–4). There were statistically significant differences between enchondroma and chondrosarcoma for both features, with deeper (greater than grade 2) and more extensive (greater than grade 2) scalloping associated with the latter diagnosis. Depth of scalloping was particularly discriminating, with chondrosarcomas demonstrating greater than grade 2 scalloping in 75% of radiographs, 90% of CT scans, and 86% of MR images. These results are in contradistinction to those for enchondromas, which revealed depth of scalloping of grade 2 or less in 91% of radiographs, 90% of CT scans, and 95% of MR images.

The presence or absence (at CT and MR imaging) and type (arcs and rings or flocculent) (at radiography and CT) of matrix mineralization were not statistically significantly different

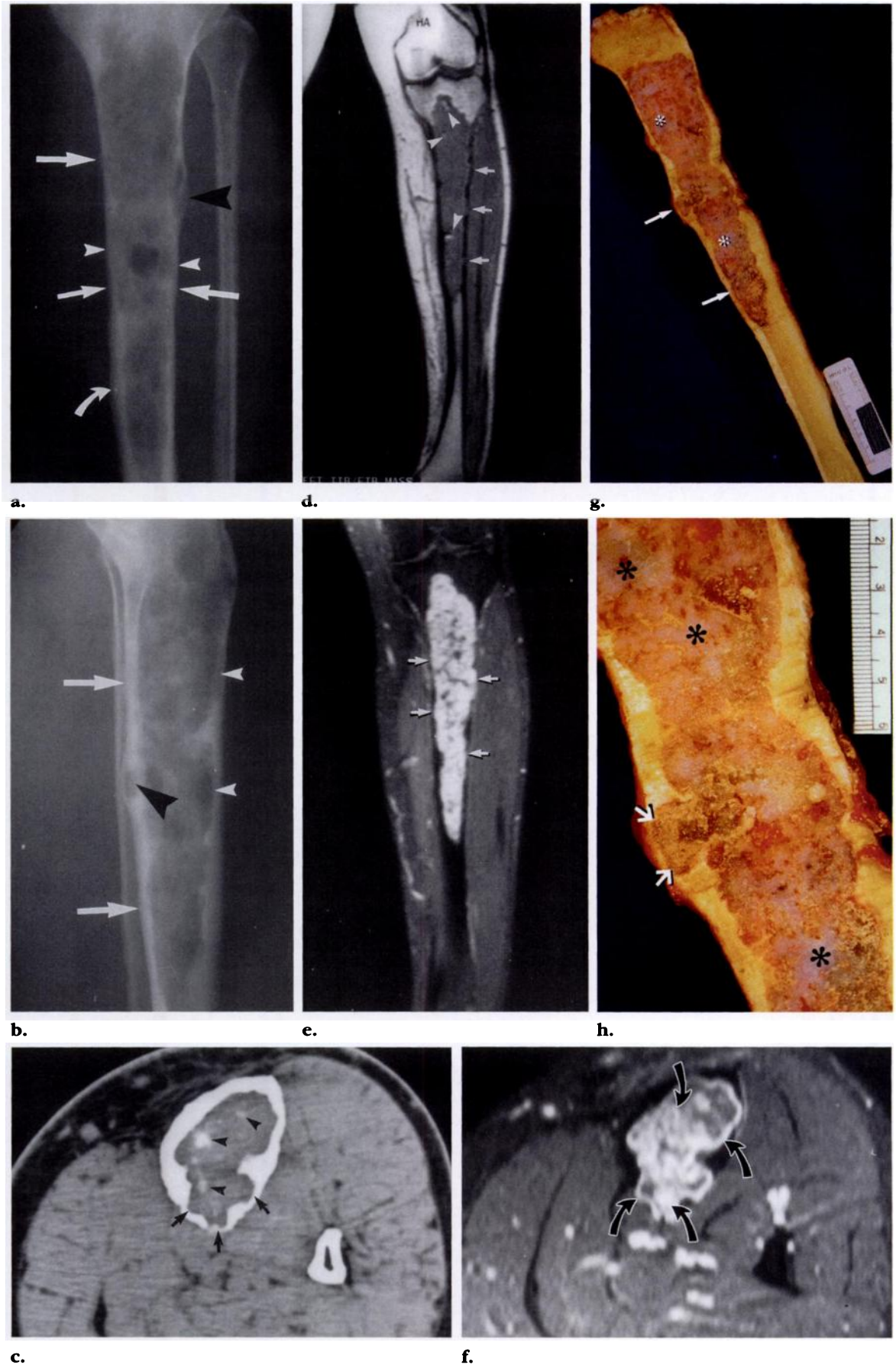
a.
d.
g.
b.
e.
h.
c.
f.

◀ **Figure 3.** Chondrosarcoma arising from enchondroma of the tibia in a 41-year-old man with a 3-year history of pain. **(a, b)** Anteroposterior **(a)** and lateral **(b)** radiographs of the proximal left tibia and fibula show a lytic lesion involving the tibial metaphysis and proximal half of the diaphysis. Deep endosteal scalloping (white arrowheads) extends over more than two-thirds of the lesion (grade 3 depth and extent). Focal cortical expansile remodeling (black arrowheads), cortical thickening (curved arrow), and focal periosteal reaction (straight arrows) are seen, but mineralized chondroid matrix is not. **(c–e)** Axial unenhanced CT **(c)**, coronal T1-weighted (500/30) MR **(d)**, and coronal inversion-recovery MR **(e)** images show irregular endosteum due to scalloping (arrows) but no extension beyond the periosteum. CT scan **(c)** reveals mineralized chondroid matrix (arrowheads). On the T1-weighted image **(d)**, the lobulated lesion has intermediate signal intensity and contains focal areas of increased signal intensity from residual areas of normal fatty marrow (arrowheads). Inversion-recovery image **(e)** shows high signal intensity within the mass and a lobular growth pattern. **(f)** Fat-suppressed, gadolinium-enhanced T1-weighted (500/30) image shows peripheral, nodular, and septal enhancement of the lesion (arrows). **(g, h)** Photograph of sagittally sectioned gross specimen **(g)** and a close-up view **(h)** show the lobular growth pattern and bluish regions of enchondroma (*) and focal areas of deep cortical invasion and endosteal scalloping (arrows) representing grade 1 chondrosarcomatous transformation. Scales are in centimeters.

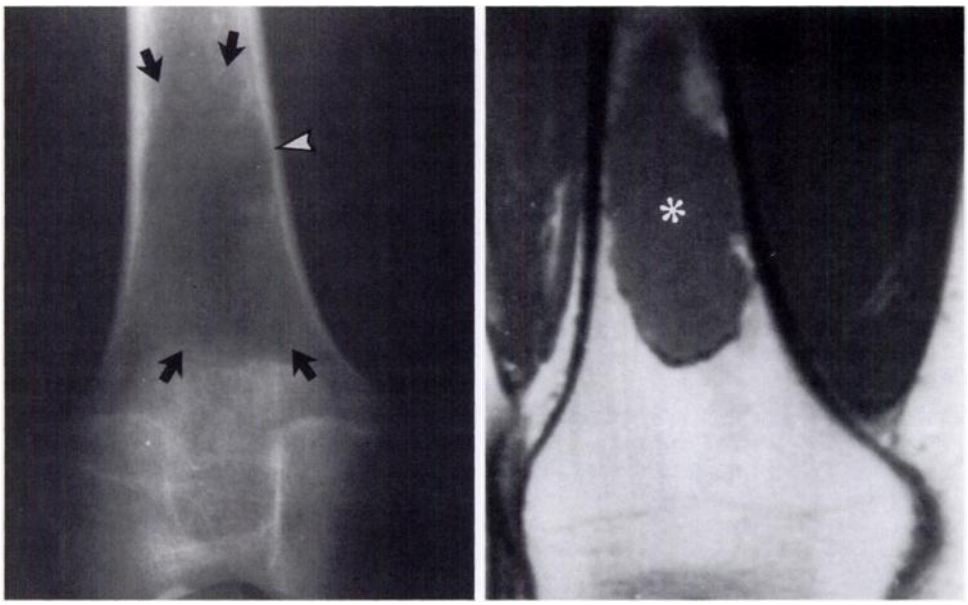

a. d.

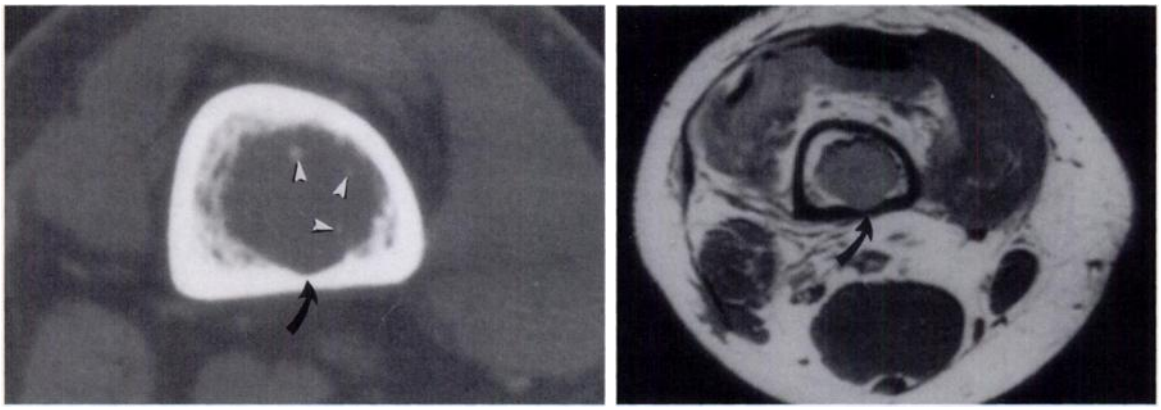

b. c.

Figure 4. Enchondroma of the distal femur in a 42-year-old woman with knee pain. **(a)** Anteroposterior radiograph of the right distal femur shows a subtle lytic lesion (arrows) with shallow endosteal scalloping focally (grade 1 depth and extent) in the medial cortex (arrowhead). **(b, c)** Axial CT **(b)** and proton density-weighted (2,100/40) MR **(c)** images show focal endosteal scalloping (grade 2) in the posterior cortex (arrow) that was not seen on the lateral radiograph (not shown). Axial unenhanced CT scan **(b)** through the distal femur reveals chondroid mineralization (arrowheads) not seen at radiography. **(d)** Coronal T1-weighted (550/20) MR image better demonstrates the lobulated margins and extent (*) of the lesion.

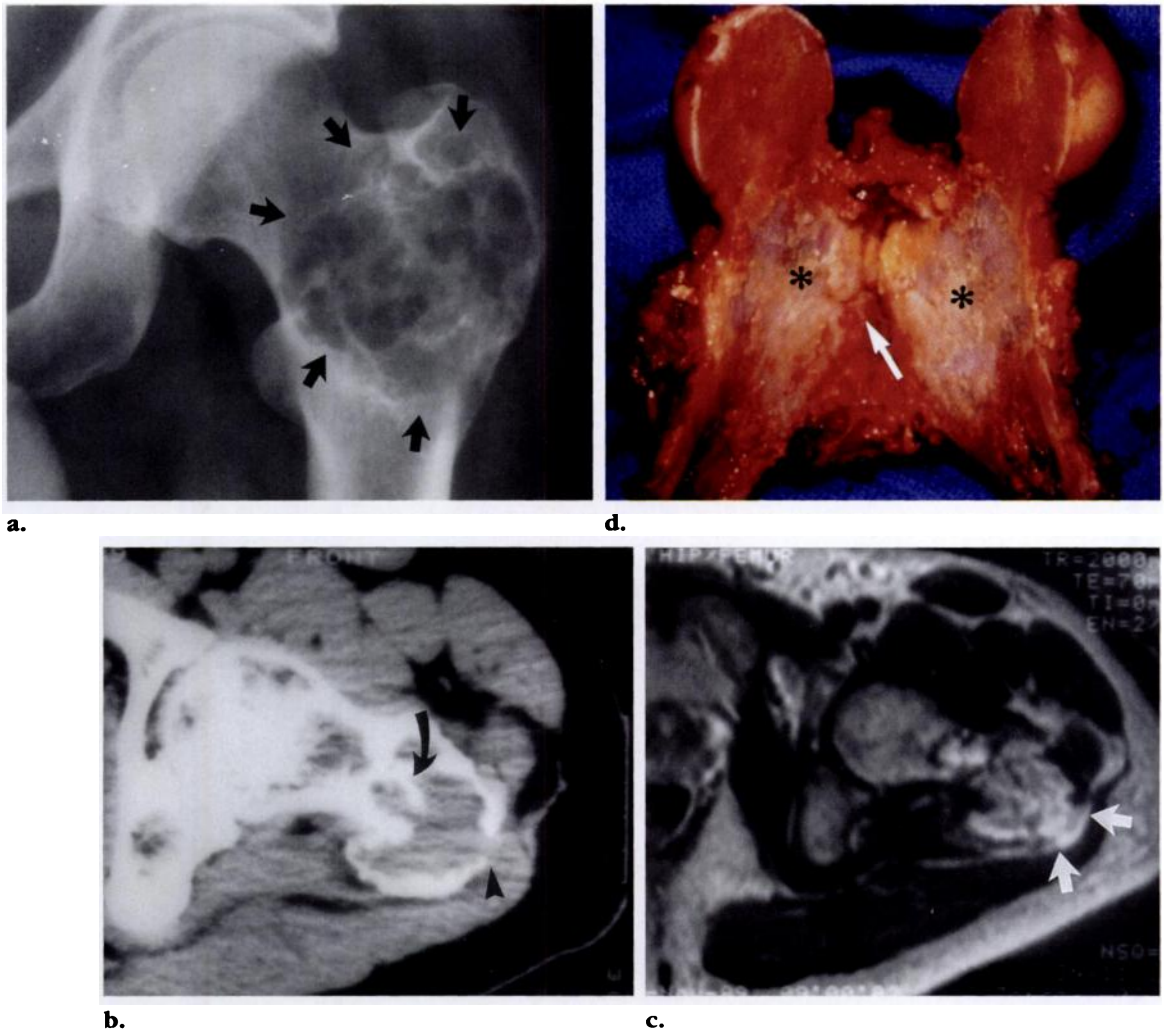

Figure 5. Chondrosarcoma of the left femur in a 37-year-old man with hip pain. **(a)** Anteroposterior radiograph of the proximal left femur reveals a multiloculated, expansile lesion (arrows) involving the intertrochanteric region. No mineralized matrix is demonstrated. **(b)** Unenhanced CT scan through the lesion shows chondroid mineralized matrix (arrow), better seen on more inferior images (not shown), and deep endosteal scalloping (grade 4 depth) (arrowhead). **(c)** Axial T2-weighted (2,500/90) MR image shows lobulated contours and hyperintense signal of the lesion. Focal soft-tissue mass (arrows) is seen at the site of cortical disruption. **(d)** Photograph of bivalved gross specimen sectioned in the coronal plane shows lobular bluish white chondroid replacement of marrow (*) and focal penetration of cortex by a small soft-tissue mass (arrow).

Table 4
Extent and Presence of Matrix Mineralization in Enchondromas and Chondrosarcomas as Depicted by Modality

Matrix Mineralization	Enchondroma	Chondrosarcoma
Extent at radiography (P = .004)*		
Grade 1	9 (10)	15 (20)
Grade 2	11 (13)	21 (28)
Grade 3	67 (77)	38 (51)
Extent at CT (P = .530)*		
Grade 1	1 (3)	3 (7)
Grade 2	4 (10)	5 (11)
Grade 3	34 (87)	38 (83)
Presence by modality		
Radiography (P = .001)	87 (95)	74 (78)
CT (P = .251)	39 (100)	46 (94)
MR imaging (P = .079)	33 (94)	26 (79)

Note.—Data are given only for those cases in which matrix mineralization was present. Numbers in parentheses are percentages, which were calculated from total for each modality.
*Grade 1 = less than one-third of lesion involved, grade 2 = one-third to two-thirds of lesion involved, grade 3 = more than two-thirds of lesion involved.

between enchondroma and chondrosarcoma (Table 4). There was a statistically significant difference between the two lesions in the radiographic presence and extent of matrix mineralization (but not at CT or MR imaging), although there was significant overlap, with enchondromas more frequently showing more prominent mineralization (Table 4). CT was superior to radiography (Figs 2–5) in depicting matrix mineralization, and both these modalities were better than MR imaging (Table 4). In fact, matrix mineralization was seen at CT in all cases of enchondromas and in 94% of chondrosarcomas. Small foci of high signal intensity were seen on T1-weighted MR images in 65% of enchondromas (Fig 6) and 32% of chondrosarcomas (Fig 3), a feature that was statistically significantly different between these lesions (P = .024).

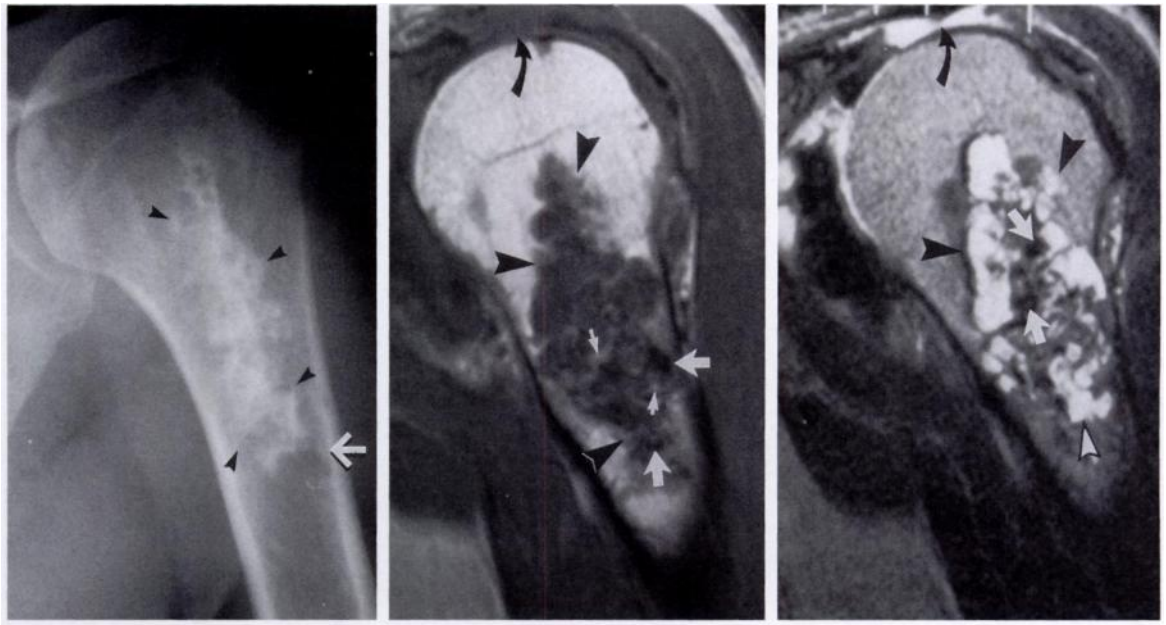

a. b. c.

Figure 6. Enchondroma of the left humerus in a 73-year-old woman with shoulder pain. **(a)** Anteroposterior radiograph demonstrates a mineralized cartilage matrix (arrowheads) in the proximal humeral diametaphysis. Focal shallow endosteal scalloping (arrow) is seen in the humeral diaphysis. **(b, c)** Coronal T1-weighted (500/25) **(b)** and T2-weighted (2,000/100) **(c)** MR images show a lobulated lesion (arrowheads) with heterogeneous signal intensity replacing the marrow. The lesion is primarily intermediate in signal intensity with T1 weighting, although focal areas of low signal intensity from mineralization (large white arrows in **b**) and high signal intensity from entrapment of residual normal fatty marrow (small arrows) are also seen. The lesion is primarily high in signal intensity with T2 weighting, with low-signal-intensity areas again secondary to mineralization (white arrows in **c**). Images reveal a full thickness rotator cuff tear (black arrow) that was responsible for the patient's pain. **(d)** Photograph of coronally sectioned gross specimen shows the mass (black *) replacing the marrow with intervening areas of normal marrow (white *).

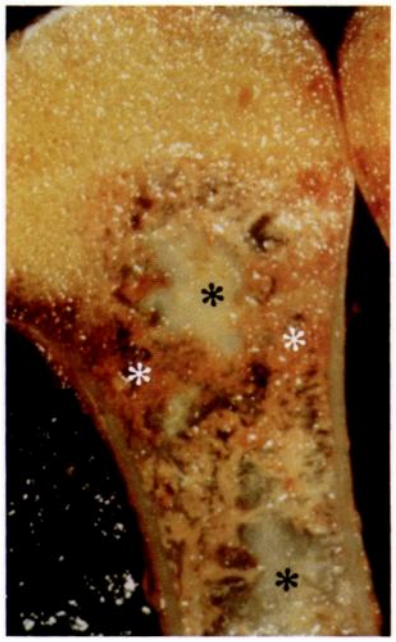

c.

The CT attenuation values and MR imaging signal intensity of the nonmineralized tumor components were similar in these lesions. At CT, all lesions had attenuation lower than or similar to that of muscle. On T1-weighted MR images, the nonmineralized component in both lesions was always of low to intermediate signal intensity; on T2-weighted images, the nonmineralized component was intermediate to high signal intensity with frequent low-signal-intensity septations in both lesions. The degree of homogeneity or heterogeneity of the nonmineralized component was also not statistically different between enchondroma and chondrosarcoma. At MR imaging, a lobulated

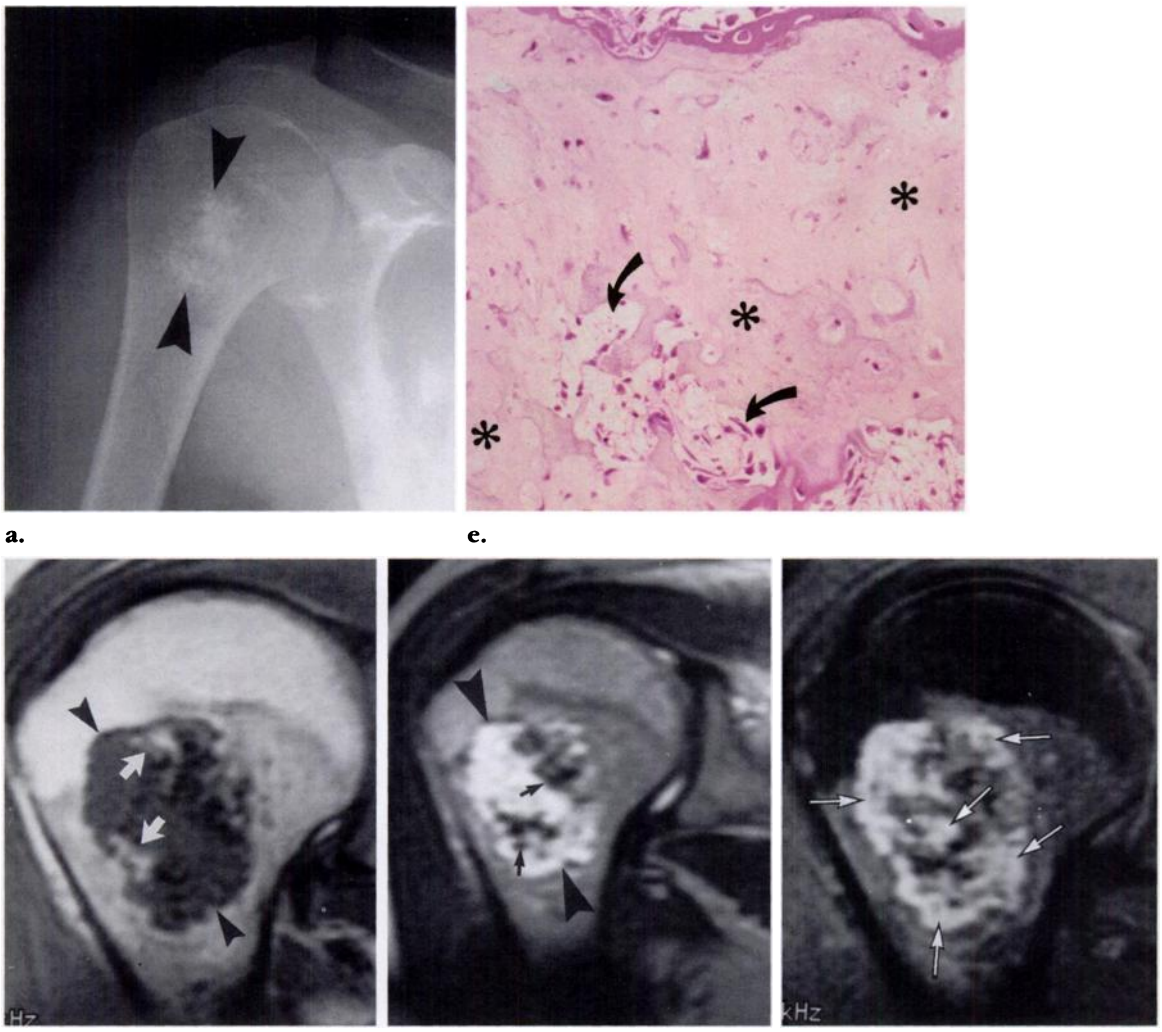

Figure 7. Enchondroma of the humerus in a 37-year-old woman with shoulder pain. **(a)** Anteroposterior radiograph shows a central lesion (arrowheads) in the proximal humeral metaphysis with chondroid mineralized matrix. **(b)** On a coronal T1-weighted (550/30) MR image, the lesion (arrowheads) displays lobulated margins and heterogeneous but predominantly intermediate signal intensity with focal areas of high signal intensity due to residual yellow marrow (arrows). **(c)** On a T2-weighted (2,000/90) image, the lesion is predominantly hyperintense with focal areas of low signal intensity representing mineralized matrix (arrows). **(d)** Fat-saturated gadolinium-enhanced coronal T1-weighted (600/17) image reveals septal, nodular, and peripheral enhancement (arrows) within the lesion. **(e)** Photomicrograph (original magnification, ×250; hematoxylin-eosin stain) shows chondroid tissue (*) surrounding islands of fatty marrow (arrows).

margin was common in both lesions (78% of enchondromas and 72% of chondrosarcomas [$P = .69$]). Neither the pattern ($P = .2$) nor the degree ($P = .38$) of enhancement after intravenous administration of gadolinium helped differentiate enchondroma from chondrosarcoma (Figs 3, 7).

Additional features that showed statistically significant differences between enchondroma and chondrosarcoma for at least one imaging modality were cortical remodeling (Fig 8), cortical destruction, pathologic fracture (Fig 9),

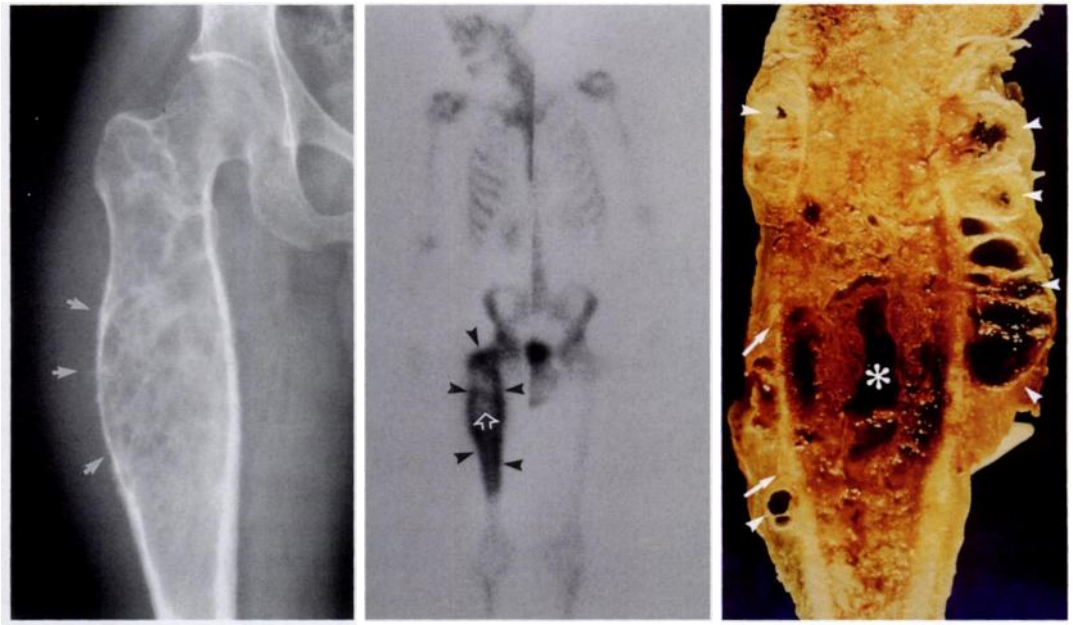

8a. 8b. 8c.

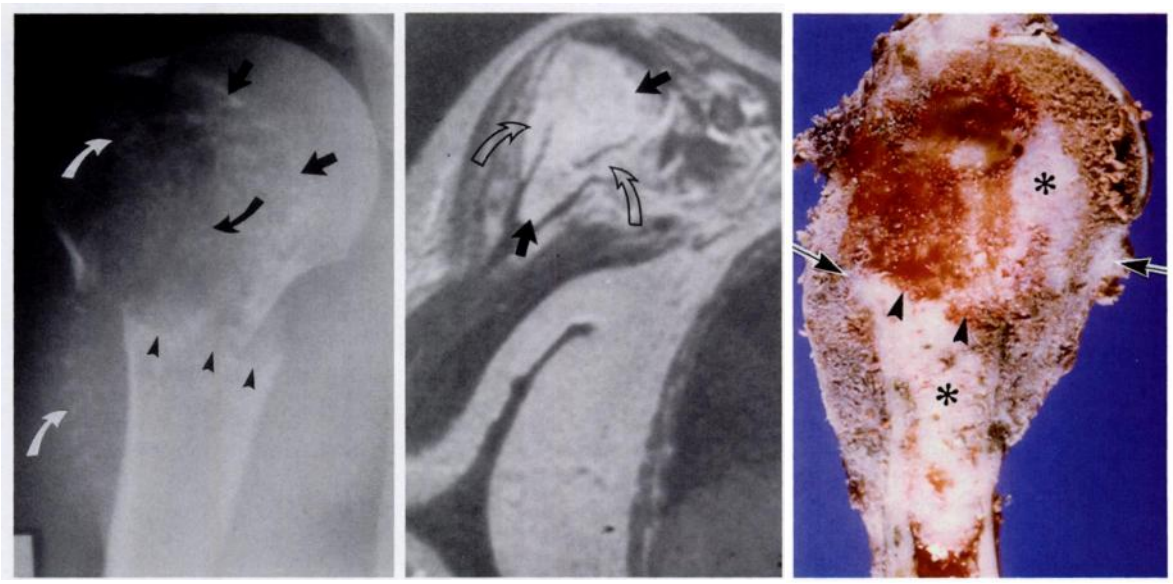

9a. 9b. 9c.

Figures 8, 9. **(8)** Chondrosarcoma (grade 3) of the femur in a 68-year-old man with pain and swelling. **(a)** Anteroposterior radiograph of the right femur shows a trabeculated lesion in the proximal diaphysis that has markedly expanded the femoral contour. Periosteal reaction is seen along the cortex (arrows). **(b)** Delayed bone scintigram shows heterogeneous, increased uptake (arrowheads) that is greater than that of the anterior superior iliac spine and central photopenia (arrow). **(c)** Photograph of coronally sectioned gross specimen shows periosteal reaction (arrows), central necrosis (*), and soft-tissue extension (arrowheads). **(9)** Chondrosarcoma of the proximal humerus in a 50-year-old woman with pathologic fracture. **(a)** Anteroposterior radiograph of the shoulder reveals a transverse fracture (arrowheads) through a lytic lesion (straight arrows) of the proximal humeral metaphysis. Chondroid mineralized matrix is seen in the lesion and soft tissues lateral to the fracture (curved arrows). **(b)** On a T2-weighted (2,000/90) coronal MR image, the lesion (solid arrows) shows hyperintense signal with extension into lateral soft tissues (open arrows). **(c)** Photograph of coronally sectioned gross specimen shows replacement of normal marrow corresponding to the lesion extent seen on MR images (*), soft-tissue extension (arrows), and healed fracture deformity (arrowheads).

Table 5
Other Significant Features of Enchondroma and Chondrosarcoma as Depicted by Modality

Imaging Finding	Enchondroma	Chondrosarcoma	*P* Value
Cortical remodeling			
Radiography	14 (15)	45 (47)	<.0005
CT	8 (21)	26 (53)	.0210
MR imaging	4 (11)	15 (45)	.0080
Cortical destruction			
Radiography	5 (5)	54 (57)	<.0005
CT	3 (8)	43 (88)	<.0005
MR imaging	1 (3)	24 (73)	<.0005
Pathologic fracture			
Radiography	5 (5)	26 (27)	.0040
CT	1 (3)	10 (20)	.0050
MR imaging	0 (0)	5 (15)	.0290
Cortical thickening			
Radiography	16 (17)	45 (47)	<.0005
CT	4 (10)	23 (47)	.0130
MR imaging	3 (9)	9 (27)	.0900
Periosteal reaction			
Radiography	3 (3)	48 (51)	<.0005
CT	8 (21)	23 (47)	.0007
MR imaging	1 (3)	5 (15)	.1780
Soft-tissue extension			
Radiography	1 (1)	44 (46)	<.0005
CT	1 (3)	29 (59)	<.0005
MR imaging	1 (3)	25 (76)	<.0005

Note.—Numbers in parentheses are percentages, which were calculated from total for each modality.

cortical thickening, periosteal reaction (Fig 8), and soft-tissue extension (Table 5) (Figs 5, 10). The largest differences in percentages of cases of enchondroma versus chondrosarcoma demonstrating these findings (Table 5) were seen with cortical destruction (at CT and MR imaging), periosteal reaction (at radiography), and soft-tissue extension (at CT and MR imaging).

There was 100% agreement between CT and MR imaging for absence of soft-tissue extension and 95% agreement for its presence. The size of the soft-tissue mass was within 1 cm at both CT and MR imaging in only 75% of cases, with

Figure 10. Chondrosarcoma of the femur in a 58-year-old man with knee pain. **(a)** Anteroposterior radiograph demonstrates a geographic lytic lesion with well-defined margins (black arrows) and periosteal reaction (white arrows) in the distal femur that extends to subchondral bone. **(b)** CT scan of the distal femur shows focal anterior cortical destruction with a soft-tissue mass (arrow) and deep endosteal scalloping posteriorly (arrowheads). **(c)** Photograph of axially sectioned whole mount specimen (hematoxylin-eosin stain) from a more proximal level than the CT scan shows cartilage matrix replacing marrow (*), anterior cortical penetration of tumor (curved arrow), and posterior endosteal scalloping (straight arrow).

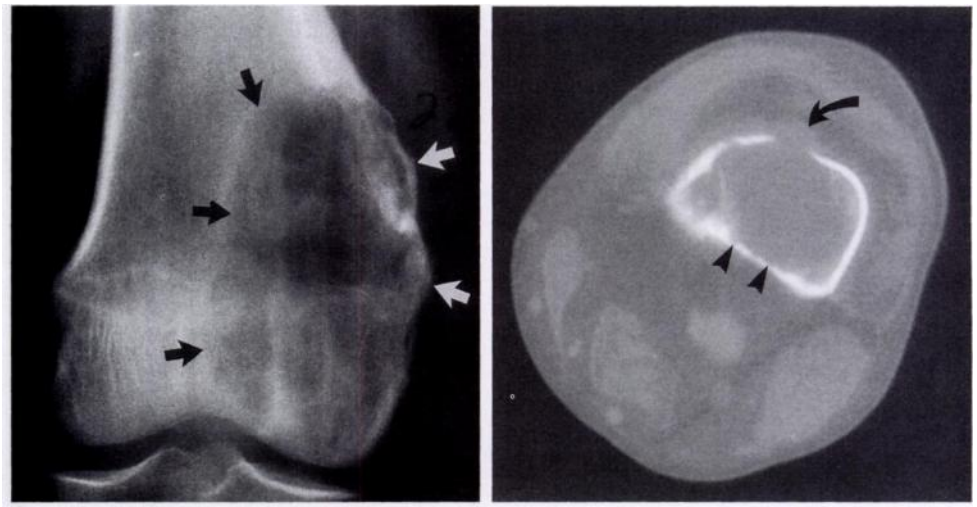

a. b.

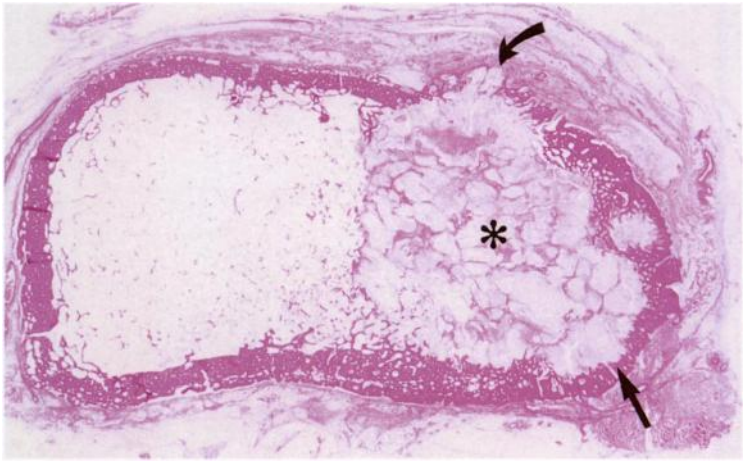

c.

the larger size estimation being demonstrated by CT. The odds ratios (ie, that a specific feature favored a diagnosis of chondrosarcoma) calculated for many of the statistically significant features are shown in Table 6.

On static bone scintigrams, there were statistically significant differences in radionuclide uptake between enchondroma and chondrosarcoma (Table 7). Enchondromas showed grade 2 or less radionuclide uptake in 79% of cases and was homogeneous in 70% (Figs 11, 12), as

Table 6
Odds Ratios for Clinical and Radiologic Features Favoring Chondrosarcoma over Enchondroma

Feature	Odds Ratio	95% Confidence Level
Sex (male)	1.9	1.1 - 3.4
Pain	4.7	1.7 - 13.2
Clinically palpable mass	11.6	5.8 - 23.3
Radionuclide uptake*	17.7	7.0 - 44.8
Depth of endosteal scalloping†		
Radiography	31.1	13.1 - 73.4
CT	77.0	19.2 - 308.4
MR imaging	92.4	16.6 - 513.6
Extent of endosteal scalloping‡		
Radiography	5.4	2.6 - 10.9
CT	7.8	3.0 - 20.4
MR imaging	7.2	3.7 - 13.9
Cortical destruction		
Radiography	22.9	8.5 - 61.6
CT	86.0	20.1 - 368.4
MR imaging	90.7	10.8 - 763.7
Cortical remodeling		
Radiography	5.0	2.5 - 10.1
CT	4.4	1.7 - 11.4
MR imaging	6.5	1.9 - 22.5
Pathologic fracture		
Radiography	6.6	2.4 - 18.0
CT	9.7	1.2 - 79.9
Cortical thickening		
Radiography	4.3	2.2 - 8.4
CT	7.7	2.4 - 25.1
MR imaging	9.0	1.0 - 16.4
Periosteal reaction		
Radiography	30.3	9.0 - 102.5
CT	3.4	1.3 - 8.9
MR imaging	6.1	0.7 - 55.0
Soft-tissue extension		
Radiography	78.5	10.5 - 586.8
CT	55.1	7.0 - 434.8
MR imaging	106.2	12.5 - 904.9

*Increased uptake greater than that of the anterior iliac crest (grade 3).
†Scalloping greater than two-thirds of cortical thickness (> grade 2).
‡Scalloping involving more than two-thirds of lesion extent (grade 3).

Table 7
Degree and Pattern of Radionuclide Uptake in Bone Scintigraphy of Enchondromas and Chondrosarcomas

Radionuclide Uptake	Enchondroma (n = 67)	Chondrosarcoma (n = 51)
Degree (P < .0005)*		
Grade 1	26 (39)	3 (6)
Grade 2	27 (40)	6 (12)
Grade 3	14 (21)	42 (82)
Pattern (P = .001)		
Homogeneous	47 (70)	19 (37)
Heterogeneous	20 (30)	32 (63)

Note.—Numbers in parentheses are percentages.
*Grade 1 = uptake less than in the anterior iliac crest, grade 2 = uptake similar to that in the anterior iliac crest, grade 3 = uptake greater than in the anterior iliac crest.

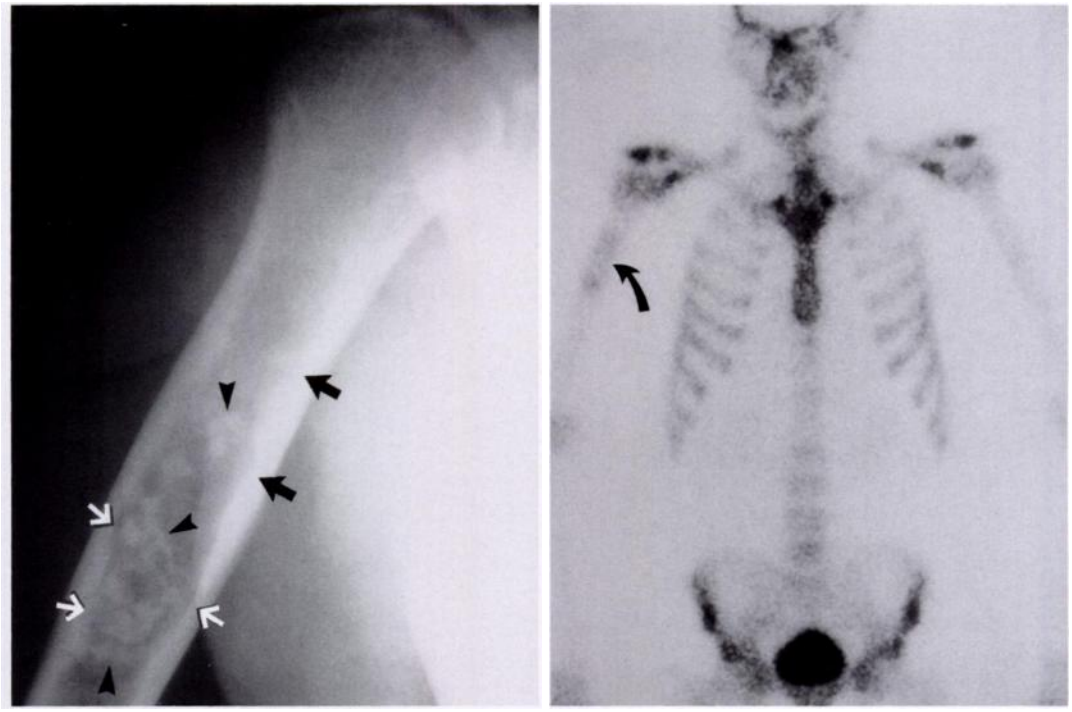

a. b.

Figure 11. Enchondroma in the proximal humerus of a 32-year-old man with shoulder pain. **(a)** Anteroposterior radiograph shows a lesion with mineralized chondroid matrix (arrowheads) and focal, shallow endosteal scalloping (grade 2 depth and extent—between one-third and two-thirds of cortical thickness and lesion extent) in the humeral diaphysis (arrows). **(b)** Delayed bone scintigram reveals faint uptake (grade 1—less than the anterior iliac crest) within the lesion (arrow).

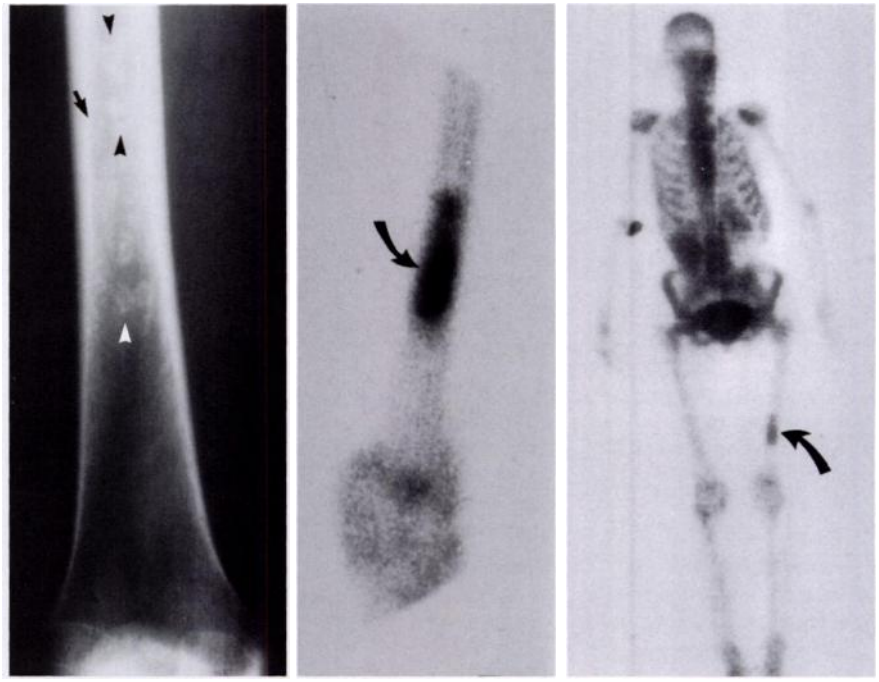

a. b. c.

Figure 12. Enchondroma of the femur in a 60-year-old woman. **(a)** Anteroposterior radiograph of the distal femoral diaphysis shows a lesion with central chondroid mineralized matrix (arrowheads) and shallow endosteal scalloping (arrow) (grade 1 depth and extent—less than one-third cortical thickness and lesion extent). **(b)** Spot view from a delayed scintigram shows the lesion (arrow) with intense radionuclide uptake. **(c)** On a whole-body scintigram, the lesion (arrow) has uptake that is less than that of the anterior iliac crest (grade 1).

Figure 13. Chondrosarcoma of the femur in a 55-year-old man with pain in the right hip. **(a)** Anteroposterior radiograph shows a long lesion involving the proximal femur with mineralized chondroid matrix (arrowheads), deep endosteal scalloping at the level of the greater trochanter (curved arrow), and focal periosteal reaction (straight arrow) in the lateral subtrochanteric region. **(b)** Delayed bone scintigram shows intense uptake (grade 3—greater than the anterior iliac crest) in the proximal portion of the lesion (solid arrow) with central photopenia (open arrow) more distally. **(c)** Photomicrograph (original magnification, ×150; hematoxylin-eosin stain) demonstrates chondroid matrix (*) engulfing bone trabecula (arrow).

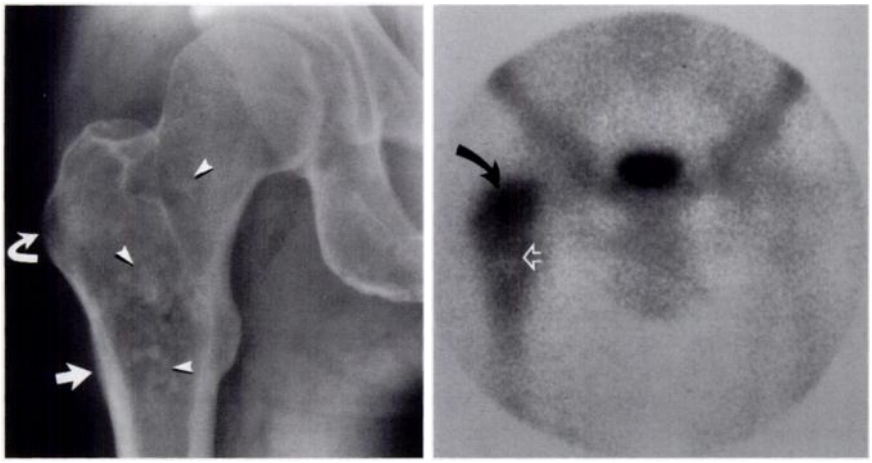

a. b.

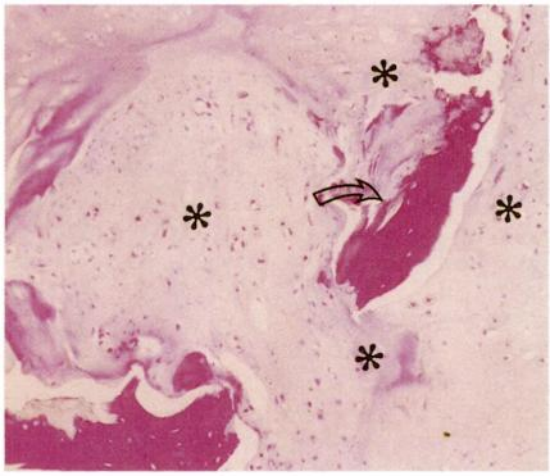

c.

opposed to chondrosarcomas, which demonstrated grade 3 uptake in 82% of cases and heterogeneity in 63% of lesions (Figs 8, 13). The extent of radionuclide uptake was similar to lesion size on radiographs in 91% of enchondromas and 80% of chondrosarcomas. Bone scintigraphic blood pool images were available in only 19 patients with enchondromas and showed uptake that was mild in 10 cases, moderate in two, and marked in one. Chondrosarcomas showed mild uptake in two cases and marked radionuclide activity in four. The *P* value for the comparison of blood pool images was .051.

According to pathologic analysis, 77 of the 92 benign lesions were classified as enchondromas (15 were considered enchondromas because they had not changed at 5 years follow-up). The 95 chondrosarcomas were classified as 35 (37%) grade 1 lesions, 29 (31%) grade 2 lesions, and 31 (33%) grade 3 lesions.

■ DISCUSSION

In our experience, the vast majority of appendicular enchondromas and chondrosarcomas (ie, those proximal to the metacarpals and metatarsals), as in the case of other bone neoplasms, can be distinguished by their clinical and radiologic features. We strongly believe this is the result of the more aggressive biologic behavior of chondrosarcoma, as seen in its pathologic appearance (16–20). The statistically significant features and those that were

Table 8
Statistical Significance of Clinical and Radiologic Features in Enchondroma and Chondrosarcoma

Statistically Significant Features	Not Statistically Significant Features
Patient age and sex	Presence of matrix mineralization
Lesion location and size	CT attenuation (nonmineralized component)
Pain	MR imaging signal intensity characteristics
Depth and extent of endosteal scalloping	Presence and pattern of gadolinium enhancement
Cortical remodeling or destruction	Lobulated margin at MR imaging
Extent of matrix mineralization	Radionuclide uptake at blood pool imaging
Cortical thickening or periosteal reaction	
Pathologic fracture	
Soft-tissue mass	
Degree and homogeneity of radionuclide uptake at bone scintigraphy	

not statistically significant in differentiating appendicular enchondroma and chondrosarcoma are shown in Table 8.

Chondrosarcoma was more common in men and older patients (mean, 1 decade older), compared with enchondroma, findings that are similar to those of previous reports (1;2, pp 25-47, 71-109;3-5;6, pp 213-224, 267-304;7, pp 268-276, 343-366). The clinical finding of a palpable mass suggests chondrosarcoma. However, in our series, 28% of patients with enchondroma had a palpable mass, a proportion similar to that reported by Geirnaerdt and coworkers (29). This finding is only partially accounted for by associated fracture and hematoma and may lead to a confusing clinical picture that should be recognized by orthopedic surgeons.

The presence of pain strongly suggests chondrosarcoma, and in fact, in our experience, it is rare for this symptom to be absent (95% of patients with chondrosarcoma experienced pain, a symptom that favors a diagnosis of malignancy 4.7 times more often than enchondroma [Table 6, odds ratios]). However, enchondroma is also commonly painful, a feature previously reported to occur in 40% of lesions and related to associated fracture that may be radiologically occult (3,27,35). In our series, the prevalence of pain with enchondroma (79% of cases) was higher than that reported in other studies. We believe this reflects a population bias related to our referral pattern, in which a greater number of cases are most likely referred to obtain a second opinion for a painful versus a painless lesion. The character of the pain in enchondroma has been reported to be different than that in chondrosarcoma, for which the pain is of longer duration and increasing severity (3,27,35). More important, in our opinion, is the question of whether the pain is related to the lesion or has another cause. Many of these chondroid neoplasms occur about the shoulder, hip, and knee, and in older patients, pain related to the joint and not the incidental enchondroma is often the cause for symptoms. We agree with Mirra (3) that conservative therapy (rest and nonsteroidal anti-inflammatory medication) will often relieve symptoms and allow pain related to chondroid lesions to be distinguished from joint-related pain. In addition, imaging frequently demonstrates joint disorders such as osteoarthritis and internal derangement (rotator cuff or meniscal tears) that cause symptoms (Figs 6, 14). Intraarticular injection of lidocaine, in our experience, may also allow distinction of joint- from lesion-related pain, since the former transiently resolves with this procedure. Pain that can be related to a chondroid neoplasm and that is not associated with identifiable fracture or intraarticular disorder is very suggestive of chondrosarcoma as opposed to enchondroma.

In our series, enchondroma and chondrosarcoma differed in lesion location. Both lesions most commonly affect the femur, humerus, and tibia. Chondrosarcomas more frequently involve the metaphysis, whereas enchondromas are more common in the diaphysis. Interestingly, an epiphyseal location is an ominous feature and strongly suggests chondrosarcoma because enchondromas are very unusual in this area (in our series, 14 of 17 epiphyseal lesions

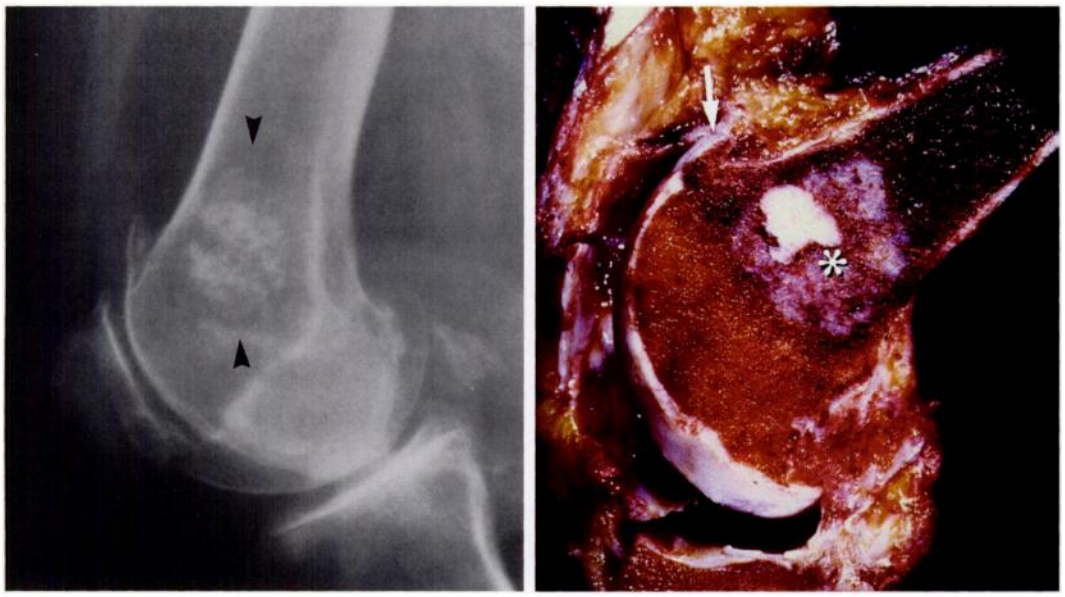

a. b.

Figure 14. Enchondroma of the distal femur in a 59-year-old woman with knee pain. **(a)** Lateral radiograph of the knee shows a chondroid lesion (arrowheads) with typical mineralized matrix in the distal femoral metaphysis and severe osteoarthritis involving the joint that was the cause of the patient's pain. **(b)** Photograph of sagittally sectioned gross specimen shows osteophyte (arrow) and lobulated marrow replacement with white and blue chondroid matrix (*).

were chondrosarcomas). This feature has not been addressed in the literature, to the best of our knowledge, and we are uncertain about the cause of this relationship. However, this observation may be helpful in differentiating between these lesions because other distinguishing features such as extent and depth of scalloping can be difficult to estimate in this area where the cortex is normally very thin (Fig 1).

Lesion sizes of enchondroma and chondrosarcoma were also different, and as expected, malignant lesions had a larger average size. Tumor size was overestimated on radiographs compared with on CT and MR images because of the difficulty in determining the exact lesion margin with radiography (Figs 1, 4). Although there is certainly overlap in size range, lesions larger than 5-6 cm in diameter are much more likely to represent chondrosarcoma (P = .001-.014, depending on modality).

The radiologic features that showed statistically significant differences between enchondroma and chondrosarcoma all reflect the underlying pathologic character of the latter entity as a more aggressive process and its resulting effects on the surrounding tissue. The imaging characteristics that should suggest chondrosarcoma are endosteal scalloping depth and extent (greater than two-thirds of cortical thickness and along more than two-thirds of the lesion), extent of matrix mineralization (within less than two-thirds of the lesion as seen on radiographs), presence of cortical remodeling or destruction and thickening, periosteal reaction, pathologic fracture, and associated soft-tissue mass. The maximum depth of scalloping (in any location and when more than two-thirds of cortical thickness) was particularly useful for discriminating between these lesions and was highly suggestive of chondrosarcoma (lesions with this finding were 31-92 times, depending on modality, more likely to be malignant [Table 6, odds ratios]). Enchondromas showed scalloping less than two-thirds of cortical thickness in 91% of cases at radiography, in 90% at CT, and in 95% at MR imaging. In contradistinction, chondrosarcomas revealed endosteal scalloping greater

than two-thirds of cortical thickness in 75% of cases at radiography, in 90% at CT, and in 86% at MR imaging. MR imaging and CT are superior to radiography for detecting focal areas of scalloping, in concordance with the recent findings of Preidler and colleagues (44), because the entire cortical circumference can be seen on cross-sectional images as opposed to only the areas seen tangentially on radiographs. The longer the extent of scalloping (relative to lesion length), the more likely the lesion represented chondrosarcoma, with 67%–79% (depending on imaging modality) of these lesions showing endosteal scalloping along more than two-thirds of the neoplasm. There was more overlap between enchondromas and chondrosarcomas with regard to the extent of scalloping, compared with the depth of scalloping, with 66%–89% (depending on imaging modality) of benign lesions showing scalloping along less than two-thirds of the lesion extent. It is possible that endosteal scalloping depth may be such a good feature for distinguishing between benign and malignant chondroid lesions because many chondrosarcomas arise from antecedent enchondromas. The areas of more aggressive growth represent the regions of malignant transformation but constitute only small foci within the entire chondroid lesion. We agree with Mirra and his colleagues (3,13,14) that this scenario is far more common than recognized; however, whereas they estimate this process accounts for 40% of chondrosarcomas, we suggest that it is even more frequent. This hypothesis is supported by the identification of regions of bland enchondroma in many chondrosarcomas. This relationship also has important implications for biopsy of cartilaginous lesions because they are often large and the question of whether the tissue retrieved is truly representative is often of concern. We believe imaging is vital to direct biopsy to the deepest area of endosteal scalloping, which will often harbor the most aggressive foci of tumor (Fig 3).

Other imaging features that also reflect the more aggressive character of chondrosarcoma and showed statistically significant differences between chondrosarcoma and enchondroma were cortical remodeling or destruction, cortical thickening, pathologic fracture, and soft-tissue mass. Contrary to our findings, Geirnaerdt and colleagues (29), in a study comparing enchondroma and grade 1 chondrosarcoma, found that many of these same features were not helpful in distinguishing between these lesions. However, we believe this different outcome is explained by variations in study design. In the study by Geirnaerdt et al (29), 51% of enchondromas were phalangeal in location, a site well known to be associated with expansile remodeling, and 35% of their chondrosarcomas were axial. As previously discussed, there is usually little diagnostic dilemma in both of these locations. In addition, we quantitatively analyzed many of these abnormalities rather than just observing their presence or absence, and evaluation was performed with multiple modalities rather than simply radiography. These factors presumably led to more extensive data to determine differences between these lesions. Soft-tissue extension has previously been reported to occur in only 25%–30% of chondrosarcomas (1;2, pp 25–47, 71–109;3,16–20,29). Our study suggests that this finding is seen more frequently (46% of cases at radiography, 59% at CT, 76% at MR imaging) and, as expected, is best evaluated with MR imaging with its superior contrast resolution. In one case of enchondroma, imaging studies revealed a soft-tissue mass that we presumed, in retrospect, was associated with fracture and hematoma.

Matrix mineralization was frequent in both enchondromas and chondrosarcomas. CT was the best modality to detect mineralization characteristic of a chondroid neoplasm, as evidenced by the fact that all enchondromas showed evidence of calcification on CT scans but only 95% revealed these areas on radiographs. At MR imaging performed with all pulse sequences, the mineralization in enchondromas was seen as nodular areas of low signal intensity and was nonspecific in appearance; it was present in 94% of these lesions. In chondrosarcomas, mineralization was seen in 94% of cases at CT and 78% at radiography and was less extensive compared with that seen in enchondroma (Table 4). We believe these lower frequencies also reflect the pathologic characteristics of chondrosarcoma and a higher degree of anaplasia with less common enchondral ossification and perhaps replacement of previous areas of enchondroma in cases of malignant degeneration.

Another feature not previously described that was more frequent in enchondroma (65% of lesions) than chondrosarcoma (35%) was the presence of speckled areas of high signal intensity on T1-weighted images. We believe these areas result from the lobular growth of enchondroma, which leaves intervening residual areas of normal yellow bone marrow, as

has been observed pathologically. This histologic feature is rare in chondrosarcoma, which infiltrates, surrounds, and obliterates marrow fat, and is the most important distinction between low-grade chondrosarcoma and enchondroma for our pathologists. We postulate that 35% of chondrosarcomas show this feature at MR imaging (contrary to histologic analysis) because of the frequent occurrence of malignancy arising in enchondroma. It is the enchondromatous component that demonstrates the speckled pattern, and it is interesting to note that the prevalence of this MR imaging finding in chondrosarcoma (35% of cases) in our study was similar to Mirra's estimate of the chondrosarcomas arising in enchondroma (40%) (3).

The lobular growth pattern seen at MR imaging in 78% of enchondromas and 72% of chondrosarcomas is typical of most chondroid neoplasms, and its prevalence is not significantly different between these lesions. De Beuckeleer and coworkers (39) found that the presence of low-signal-intensity septa on T2-weighted MR images was also suggestive of chondrosarcoma (5 of 5 lesions), although 56% of enchondromas (9 of 16) also showed this pattern. We did not find this MR imaging pattern to be helpful for differentiating enchondroma from chondrosarcoma, since low signal intensity was seen about cartilage lobules in both lesions and pathologically corresponded to enchondral ossification or fibrous septations. Janzen et al (45) reported the finding of edema about chondrosarcoma (as opposed to enchondroma) margins on inversion-recovery MR images. Although we had relatively few such MR images and did not specifically search for this finding, we have seen cases of chondrosarcoma (Fig 3) without this abnormality. In addition, we would be concerned that enchondromas could have surrounding edema associated with fracture.

Previous reports have described the gadolinium enhancement pattern of chondroid neoplasms and suggested that enchondromas show peripheral enhancement versus the septal or more diffuse enhancement seen in chondrosarcomas (29,32,33,39). In our study, neither the pattern ($P = .2$) nor degree ($P = .38$) of enhancement helped differentiate enchondroma from chondrosarcoma (Figs 3, 7). This finding correlates with the fact that pathologists do not use vascularity as a criterion to distinguish between these lesions (3,5,41,42). Our findings are similar to those of Aoki and colleagues (32), who characterized enchondromas and chondrosarcomas as having a arc and ring pattern of enhancement (septal and peripheral). Geirnaerdt and coworkers (29), on the other hand, found septal enhancement only in chondrosarcomas but had no enchondromas in their series for comparison. De Beuckeleer and colleagues (39) also found this pattern of enhancement to be more common in chondrosarcomas, although it was seen in only 50% of cases and in 23% of enchondromas. Preliminary studies of MR imaging performed with dynamic enhancement have also suggested early enhancement of chondrosarcoma as a possible useful discriminating feature of malignant versus benign cartilage lesions (46). Further evaluation of this technique may prove helpful, although we still harbor concerns about its usefulness in differentiating between these lesions based on our pathologic experience with low-grade chondrosarcoma.

Bone scintigraphy showed greater radionuclide uptake in lesion compared with the anterior iliac crest in 82% of chondrosarcomas, with heterogeneity seen in 63%. Enchondroma more often demonstrated equal or lower activity than did the anterior iliac crest in 79% of cases and homogeneity in 70%. This differentiation was statistically significant ($P < .0005$) and also reflects the higher degree of biologic activity in chondrosarcoma. We agree with Hudson and coworkers (34) in that we have not seen an intramedullary chondrosarcoma without clearly increased uptake at bone scintigraphy. In evaluation of the degree of radionuclide uptake, images with wide windows are more helpful for comparing the lesion activity with the uptake in the anterior iliac crest. Whole-body views are also preferable, in our experience, because spot views can artifactually appear to increase the degree of radionuclide activity in the lesion (Fig 12). Lack of a statistically significant difference between lesions on blood pool images again likely reflects the limited use of vascularity in distinguishing between these lesions.

Limitations of this study include its retrospective nature and lack of control (because of our referral population) of specific imaging parameters. We also did not separate different grades of chondrosarcoma and compare imaging parameters in this study to specifically address the issue of grade 1 chondrosarcoma versus enchondroma. We believe it is important to

have a solid baseline of quantitative analysis of imaging findings in a large group of chondrosarcomas and enchondromas (simulating how patients present clinically), although future projects include separately evaluating these malignancies by grade. Finally, there is not universal agreement among pathologists as to histologic criteria for low-grade chondrosarcoma, although the vast majority of our cases were reviewed by one orthopedic pathologist with more than 30 years of experience, which allowed relative internal consistency.

■ CONCLUSIONS

In conclusion, we have comparatively analyzed a large series of appendicular (proximal to the metacarpals and metatarsals) enchondromas and intramedullary chondrosarcomas. Our statistical analysis suggests that the vast majority of these lesions can be confidently diagnosed as chondroid neoplasms with identification of mineralized matrix, particularly at CT (100% of enchondromas, 94% of chondrosarcomas). In addition, multiple clinical and imaging factors (Tables 6, 8)—particularly pain related to the lesion, depth of scalloping greater than two-thirds of cortical thickness, cortical destruction and soft-tissue mass (at CT or MR imaging), periosteal reaction (at radiography), and greater uptake than the anterior iliac crest at bone scintigraphy—strongly suggest the diagnosis of chondrosarcoma. Distinction between appendicular enchondroma and chondrosarcoma can be made on the basis of these criteria in at least 90% of cases. Features for which the odds ratios strongly favor the diagnosis of malignancy include endosteal scalloping greater than two-thirds of cortical thickness at CT or MR imaging, cortical destruction at MR imaging, and soft-tissue extension at MR imaging; the presence of these features makes the diagnosis of chondrosarcoma 77, 92, 91, and 106 times more likely than enchondroma (Table 6), respectively. Future ongoing studies conducted with a multifactorial analysis should allow development of an algorithm based on these quantitative data. In addition, we intend to separately evaluate the distinction of enchondroma and grade of chondrosarcoma (with particular emphasis on grade 1 lesions) with these imaging and clinical parameters.

Acknowledgments: We gratefully thank Phyllis M. Hickey, MA, and Cindy McDonald, SrA, USAF, for the preparation of the manuscript and Robbin S. Howard, MA, for statistical analysis. In addition, we thank all past, present, and future attendees of the radiologic pathology course at the Armed Forces Institute of Pathology for providing materials that make such projects possible.

■ REFERENCES

1. Mulder JD, Kroon HM, Schutte HE, Taconis WK, eds. Radiologic atlas of bone tumors. Amsterdam, The Netherlands: Elsevier, 1993; 7-421.
2. Unni KK. Enchondroma and chondrosarcoma. In: Unni KK, ed. Dahlin's bone tumors: general aspects and data on 11,087 cases. 5th ed. Philadelphia, Pa: Lippincott-Raven, 1996.
3. Mirra JM. Intramedullary cartilage and chondroid-producing tumors. In: Mirra JM, ed. Bone tumors: clinical, radiologic, and pathologic correlations. Philadelphia, Pa: Lea & Febiger, 1989; 439-535.
4. Lichtenstein L, Jaffe HL. Chondrosarcoma of the bone. Am J Pathol 1943; 19:553-589.
5. Ragsdale BD, Sweet DE, Vinh TN. Radiology as gross pathology in evaluating chondroid lesions. Hum Pathol 1989; 20:930-951.
6. Campanacci M. Bone and soft tissue tumors. New York, NY: Springer-Verlag, 1990.
7. Huvos AG. Solitary enchondroma, chondrosarcoma, and spindle-cell chondrosarcoma (dedifferentiated chondrosarcoma). In: Mitchell J, ed. Bone tumors: diagnosis, treatment, and prognosis, 2nd ed. Philadelphia, Pa: Saunders, 1991.
8. Jaffe HL, Lichtenstein L. Solitary benign enchondroma of bone. Arch Surg 1943; 46:480-493.
9. Jaffe HL. Tumors and tumorous conditions of the bones and joints. Philadelphia, Pa: Lea & Febiger, 1958; 315-340.
10. Resnick D, Kyriakos M, Greenway GD. Tumors and tumor-like lesions of bone: imaging and pathology of specific lesions. In: Resnick D, ed. Diagnosis of bone and joint disorders. 3rd ed. Philadelphia, Pa: Saunders, 1995.
11. Crim JR, Seeger LL. Diagnosis of low-grade chondrosarcoma. Radiology 1993; 189:503-504.
12. Sanerkin NG. The diagnosis and grading of chondrosarcoma of bone: a combined cytologic and histologic approach. Cancer 1980; 45:582-594.
13. Mirra JM, Gold R, Downs J, Eckardt JJ. A new histologic approach to the differentiation of enchondroma and chondrosarcoma of the bones: a clinicopathologic analysis of 51 cases. Clin Orthop 1985; 201:214-237.
14. Mirra JM. Clinical guidelines for differentiating enchondroma from chondrosarcoma. Complications Orthop 1987; 2:89-107.
15. Dietlein M, Feaux de Lacroix W, Neufang KFR, Steinbrich W, Schmidt J. Assessment of the tumor status of cartilaginous tumors of the long tubular bones: radiological and pathological aspects. Fortschr Rontgenstr 1990; 43:174-180.
16. Pritchard DJ, Lunke RJ, Taylor WF, Dahlin DC, Medley BE. Chondrosarcoma: clinicopathologic and statistical analysis. Cancer 1980; 45:149-157.
17. Evans HL, Ayala AG, Romsdahl MM. Prognostic factors in chondrosarcoma of bone: a clinico-

pathologic analysis with emphasis on histologic grading. Cancer 1977; 40:818-831.
18. Mankin HL, Cantley KP, Lippiello L, Schille AL, Campbell CJ. The biology of human chondrosarcoma. I. Description of cases, grading, and biochemical analyses. J Bone Joint Surg [Am] 1980; 62:160-176.
19. Mankin HL, Cantley KP, Lippiello L, Schille AL, Campbell CJ. The biology of human chondrosarcoma. II. Variation in chemical composition among types and subtypes of benign and malignant cartilage tumors. J Bone Joint Surg [Am] 1980; 62:176-188.
20. Sweet DE, Madewell JE, Ragsdale BD. Radiologic and pathologic analysis of solitary bone lesions. III. Matrix patterns. Radiol Clin North Am 1981; 19:785-814.
21. Reiter FB, Ackerman LV, Staple TW. Central chondrosarcoma of the appendicular skeleton. Radiology 1972; 105:525-530.
22. Geirnaerdt MJA, Bloem JL, Eulderink F, Hogendoorn PCW, Taminiau AHM. Cartilaginous tumors: correlation of gadolinium-enhanced MR imaging and histopathologic findings. Radiology 1993; 186:813-817.
23. West OC, Reinus WR, Wilson AJ. Quantitative analysis of the plain radiographic appearance of central chondrosarcoma of bone. Invest Radiol 1995; 30:440-447.
24. Rosenthal DI, Schiller AL, Mankin HJ. Chondrosarcoma: correlation of radiological and histological grade. Radiology 1984; 150:21-26.
25. Mayes GB, Wallace S, Bernardino ME. Computed tomography of chondrosarcoma. CT 1981; 5: 345-348.
26. Lodwick GS. The radiologist's role in the management of chondrosarcoma (editorial). Radiology 1984; 150:275.
27. Brien EW, Mirra JM, Kerr R. Benign and malignant cartilage tumors of bone and joint: their anatomic and theoretical basis with an emphasis on radiology, pathology, and clinical biology. I. The intramedullary cartilage tumors. Skeletal Radiol 1997; 26:325-353.
28. Varma DGK, Ayala AG, Carrasco CH, et al. Chondrosarcoma: MR imaging with pathologic correlation. RadioGraphics 1992; 12:687-704.
29. Geirnaerdt MJA, Hermans J, Bloem JL, et al. Usefulness of radiology in differentiating enchondroma from central grade I chondrosarcoma. AJR 1997; 169:1097-1104.
30. Lodwick GS, Wilson AJ, Farrell C, Virtama P, Ditrich F. Determining growth rates of focal lesions of bone from radiographs. Radiology 1980; 134:577-583.
31. Cohen EK, Kressel HY, Frank TS, et al. Hyaline cartilage-origin bone and soft-tissue neoplasms: MR appearance and histologic correlation. Radiology 1988; 167:477-481.
32. Aoki J, Sone S, Fujioka F, et al. MR of enchondroma and chondrosarcoma: rings and arcs of Gd-DTPA enhancement. J Comput Assist Tomogr 1991; 15:1011-1016.
33. De Beuckeleer LHL, De Schepper AMA, Ramon F. Magnetic resonance imaging in cartilaginous tumors: is it useful or necessary? Skeletal Radiol 1996; 25:137-141.
34. Hudson TM, Chew FS, Manaster BJ. Radionuclide bone scanning of medullary chondrosarcoma. AJR 1982; 139:1071-1076.
35. Moser RP Jr, Gilkey FW, Madewell JE. Enchondroma. In: Moser RP Jr, ed. Cartilaginous tumors of the skeleton. Philadelphia, Pa: Hanley & Belfus, 1990; 8-35.
36. Hudson TH, Moser RP Jr, Gilkey FW, Aoki J. Chondrosarcoma. In: Moser RP Jr, ed. Cartilaginous tumors of the skeleton. Philadelphia, Pa: Hanley & Belfus, 1990; 155-205.
37. Walker CW, Moore TE. MR imaging of hyaline cartilage-containing tumors. Appl Radiol 1998; April, 20-26.
38. Janzen L, Logan PM, O'Connell JX, Connell DG, Munk PL. Intramedullary chondroid tumors of bone: correlation of abnormal peritumoral marrow and soft-tissue MRI signal with tumor type. Skeletal Radiol 1997; 26:100-106.
39. De Beuckeleer LHL, De Schepper AMA, Ramon F. Magnetic resonance imaging of cartilaginous tumors: retrospective study of 79 patients. Eur J Radiol 1995; 21:34-40.
40. Hudson TM, Manaster BJ, Springfield DS, et al. Radiology of medullary chondrosarcoma: preoperative treatment planning. Skeletal Radiol 1983; 10:69-78.
41. Lagergren C, Linbom A, Soderberg G. The blood vessels of chondrosarcomas. Acta Radiol 1961; 55:321-328.
42. Yaghmai I. Angiographic features of chondromas and chondrosarcomas. Skeletal Radiol 1978; 3:91-98.
43. Moses LE, Emerson JD, Hosseini H. Analyzing data from ordered categories. N Engl J Med 1984; 311:442-448.
44. Preidler KW, Brossmann J, Daenen B, et al. Measurements of cortical thickness in experimentally created endosteal bone lesions: a comparison of radiography, CT, MR imaging, and anatomic sections. AJR 1997; 168:1501-1505.
45. Janzen L, Logan PM, O'Connell JX, Connell DG, Munk PL. Intramedullary chondroid tumors of bone: correlation of abnormal peritumoral marrow and soft-tissue MRI signal with tumor type. Skeletal Radiol 1997; 26:100-106.
46. Geirnaerdt MJ, Bloem JL, Van Der Woode H, Taminiau AH, Hogendoorn PC. Fast dynamic contrast-enhanced subtraction MR imaging allows differentiation of benign and low-grade malignant cartilaginous tumors (abstr). Radiology 1996; 201(P):359.

This article meets the criteria for 1.0 credit hour in Category 1 of the AMA Physician's Recognition Award. To obtain credit, see the questionnaire on pp 1239-1246.